

Spin Dynamics of the 2D Spin $\frac{1}{2}$ Quantum Antiferromagnet Copper Deuterioformate Tetradeuterate (CFTD)

H. M. Rønnow,^{1,2} D. F. McMorrow,¹ R. Coldea,^{3,4} A. Harrison,⁵ I. D. Youngson,⁵ T. G. Perring,⁴ G. Aeppli,⁶ O. Syljuåsen,⁷ K. Lefmann,¹ and C. Rischel⁸

¹*Condensed Matter Physics and Chemistry Department, Risø National Laboratory, DK-4000 Roskilde, Denmark*

²*DRFMC, CEA, 17, Rue des Martyrs, 38054 Grenoble, France*

³*Solid State Division, Oak Ridge National Laboratory, Oak Ridge, Tennessee 37831*

⁴*ISIS facility, Rutherford Appleton Laboratory, Didcot, United Kingdom*

⁵*Department of Chemistry, University of Edinburgh, The King's Buildings, Edinburgh EH9 3JJ, United Kingdom*

⁶*NEC Research, 4 Independence Way, Princeton, New Jersey 08540*

⁷*NORDITA, Copenhagen, Denmark*

⁸*Niels Bohr Institute, Copenhagen, Denmark*

(Received 28 September 2000; published 28 June 2001)

The magnetic excitation spectrum in the two-dimensional (2D) $S = 1/2$ Heisenberg antiferromagnet copper deuterioformate tetradeuterate has been measured for temperatures up to $T \sim J/2$, where $J = 6.31 \pm 0.02$ meV is the 2D exchange coupling. For $T \ll J$, a dispersion of the zone boundary energy is observed, which is attributed to a wave vector dependent quantum renormalization. At higher temperatures, spin-wavelike excitations persist, but are found to broaden and soften. By combining our data with numerical calculations, and with existing theoretical work, a consistent description of the behavior of the model system is found over the whole temperature interval investigated.

DOI: 10.1103/PhysRevLett.87.037202

PACS numbers: 75.10.Jm, 05.70.Jk, 75.50.Ee

While at the atomic level, magnetism is a quantum phenomenon, the collective behavior of magnets can be largely understood using classical concepts. This can even be true for antiferromagnets with low spin and spatial dimensionality, where quantum fluctuations are sizable. A famous example is the 2D quantum ($S = 1/2$) Heisenberg antiferromagnet on a square lattice (2DQHAFSL) with nearest-neighbor interactions. Considerable effort has been devoted to this particular model because it describes the parent compounds of the high- T_c superconducting cuprates, and also because it once was thought to have a spin fluid rather than a Néel ground state.

By now, it is well established that at zero temperature the 2DQHAFSL displays long-range order, albeit with a staggered moment reduced by quantum fluctuations [1]. In addition, harmonic spin-wave (SW) theory, based on a classical image of the spins as coupled precessing tops, gives an excellent account of the spin dynamics up to intermediate frequencies at $T = 0$. At finite temperatures, long-range order is destroyed by thermal fluctuations, and the system possesses short-range order only, characterized by a temperature-dependent correlation length $\xi(T)$. A combination of low-temperature renormalized classical theory [2], intermediate temperature quantum Monte Carlo (QMC) [3,4] and high-temperature methods [5,6], accounts for the experimental data for $\xi(T)$, covering the range $J/5 < T \lesssim J$ [7–11]. Thus, a coherent picture exists for the thermodynamic properties at all temperatures for $S = 1/2$, as well as for higher values of the spin [12]. The remaining questions about the 2DQHAFSL concern the intermediate and low frequency spin dynamics at nonzero T , and the high frequency spin dynamics at all T .

In both cases one could well expect to see more severe quantum effects because they should be more sensitive than the static properties to the nonlinearities of Heisenberg's equations for a low spin system. The present paper describes the first experiment to confront all of these questions directly over the full energy scale set by J .

Though experiments on the dynamics of the 2DQHAFSL are relatively scarce, considerable theoretical work exists. Time dependent information is contained in the dynamical structure factor $S(Q, \omega) = \int dt e^{-i\omega t} \sum_r e^{iQr} \langle S_0(0) S_r(t) \rangle$, which is a function of wave vector Q and energy $\hbar\omega$, and is measured directly in neutron scattering experiments. The $T = 0$ properties can be described by classical SW theory, but with quantities such as the SW velocity $v_s = Z_c \sqrt{2} J a$, spin stiffness $\rho_s = Z_\rho J/4$, and susceptibility $\chi_\perp = Z_\chi/(8J)$ renormalized by quantum corrections. Consistent values for the renormalization constants $Z_c = 1.18$, $Z_\rho = 0.72$, and $Z_\chi = 0.51$ have been obtained using the SW expansion to order $1/(2S)^2$ [1], and series expansion from the Ising limit [13]. However, these two approaches to the $T = 0$ spin dynamics disagree in detail, in that the SW expansion predicts a constant energy at the zone boundary (ZB), whereas the Ising-limit expansion predicts a $\sim 7\%$ dispersion.

On warming, scattering from thermally excited magnons, and a variation of the order parameter on a length scale set by ξ , will limit the lifetime of the excitations. Correspondingly, the inverse magnon lifetime, Γ , will increase, while the dispersion softens to lower energies. Various theoretical studies [14–21] and QMC calculations in the limited temperature range

$0.35J < T < 0.5J$ [22] have addressed the dynamic structure factor of the 2DQHAFSL at finite T . Most approaches agree on the existence of well-defined excitations, but few experimental data are available to test the various quantitative predictions. Much of the experimental work on the 2DQHAFSL has focused on La_2CuO_4 [7,8] and $\text{Sr}_2\text{CuCl}_2\text{O}_2$ [9,23], both of which contain the CuO_2 planes that are the building blocks of the cuprates. These materials have the drawback that their large coupling constant $J \sim 1500$ K makes studies on temperature and energy scales comparable to J technically challenging. Another realization of the 2DQHAFSL is $\text{Cu}(\text{DCOO})_2 \cdot 4\text{D}_2\text{O}$ (CFTD), where the $S = 1/2$ Cu moments are coupled through formate groups, leading to an exchange energy ($J = 73.2$ K) which is more amenable to experiments. The correlation length $\xi(T)$ in CFTD has recently been measured up to temperatures of $T \sim J$ [10,11], and found to be in good agreement with theory and computations.

Below 236 K, CFTD has the $P2_1/n$ space group with lattice parameters $a = 8.113$ Å, $b = 8.119$ Å, $c = 12.45$ Å, and a monoclinic angle $\beta = 101.28^\circ$. The ab plane contains face centered $S = 1/2$ Cu^{2+} ions, forming an almost square lattice. The SW dispersion along a^* and b^* measured by neutron scattering is well described by an isotropic nearest-neighbor coupling $J = 6.31$ meV, and a small anisotropy induced gap of 0.38 meV at the zone center [24]. The interlayer coupling is estimated to be less than $10^{-4}J$, while a Dzyaloshinskii-Moriya term $J_D = 0.46$ meV has been inferred from magnetization measurements [25]. Below $T_N = 16.54$ K the system orders three dimensionally due to the interlayer coupling [26].

Our neutron inelastic scattering experiments use the direct geometry time-of-flight (TOF) spectrometer HET at ISIS, U.K. The incident energy $E_i = 25$ meV gave an energy resolution of FWHM 1.64 meV at zero energy transfer. A 3.71 g single crystal of CFTD was aligned with the 2D planes normal to the incident beam. In the geometry used, the horizontal and vertical detector banks measured scattering along the $[1, 1]$ -type direction, while the diagonal banks collected data along the $[1, 0]$ directions. The measured intensities were corrected for detector efficiency, and converted to absolute units by normalizing to the incoherent scattering from a vanadium standard.

Data were collected at several temperatures between 8 and 150 K with typically 24 h of counting per temperature. The data at 8 K (within the 3D ordered phase) provide a precise determination of the spin Hamiltonian, and allow characterization of the phonon background. For example, the band at 20 meV is probably due to the localized motion of the crystal bound water, which freezes in an antiferroelectric transition at 236 K ~ 20.3 meV [26], while the extra scattering around 7 meV is due to acoustic phonons emerging from the $(1, 0, 1)$ -type reciprocal lattice points; see Fig. 1(a).

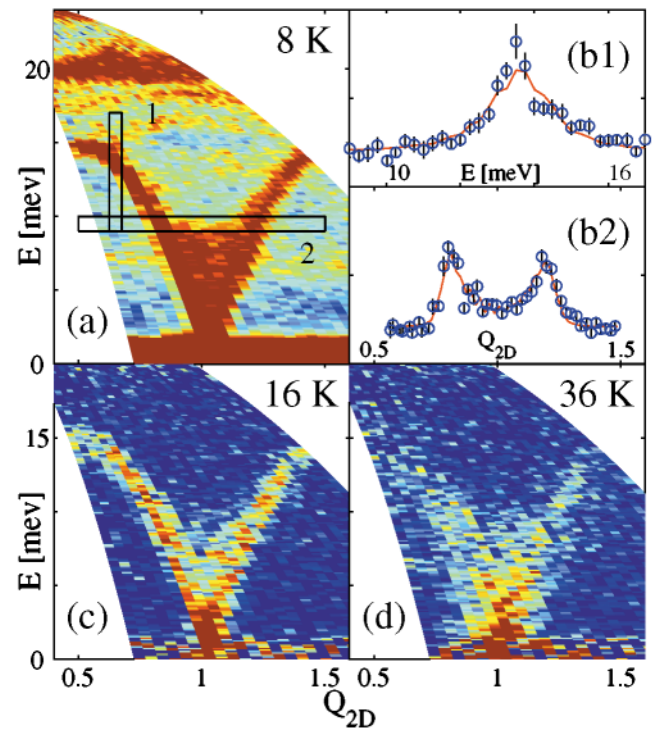


FIG. 1 (color). Inelastic TOF data from CFTD with Q_{2D} in units of (π, π) . (a) Raw data at 8 K. (b) Representative cuts along energy (b1) and Q (b2) as indicated by the windows in panel (a). The vertical scales cover 0 to 100 mbarn steradian $^{-1}$ meV $^{-1}$ spin $^{-1}$, and the solid lines are fits to the resolution convoluted cross section described in the text. (c),(d) Background subtracted data at 16 and 36.2 K, respectively. The pseudocolor scale (from blue to dark red) ranges from 0 to 50 mbarn steradian $^{-1}$ meV $^{-1}$ spin $^{-1}$.

At 8 K, the magnetic signal is concentrated along a sharp SW dispersion curve. The data were analyzed by taking cuts along Q and ω , as illustrated in Fig. 1(b), allowing the phonon contribution to be dealt with as a local background. Each cut was fitted with a parametrized model for the scattering obtained by convolving the full instrumental resolution with the linear SW theory form $S(Q, \omega) = \frac{A}{2} \sqrt{(1 - \gamma_Q)/(1 + \gamma_Q)} \delta(\omega - \omega_Q)$; $\omega_Q = 2\tilde{J}\sqrt{1 - \gamma_Q^2}$; $\gamma_Q = \frac{1}{2}(\cos Q_x + \cos Q_y)$, multiplied by the magnetic form factor of free Cu^{2+} and the Bose population factor. Since the parametrization is applied only locally (the parameters A and \tilde{J} were allowed to vary for each cut), it imposes no constraints on the global form of $S(Q, \omega)$ or on the extracted dispersion, shown in Fig. 2. It is evident that along $[1, 1]$ the dispersion is well described by a uniform renormalization of the linear SW theory result. A fit gave $J = \tilde{J}/Z_c = 6.31 \pm 0.02$ meV, in good agreement with previous neutron scattering [24] studies and the value derived from high-temperature susceptibility [25]. The present data can be combined with the susceptibility data to give a value of the renormalization factor $Z_c = 1.21 \pm 0.05$, within error the same as the theoretical value 1.18 [1,13].

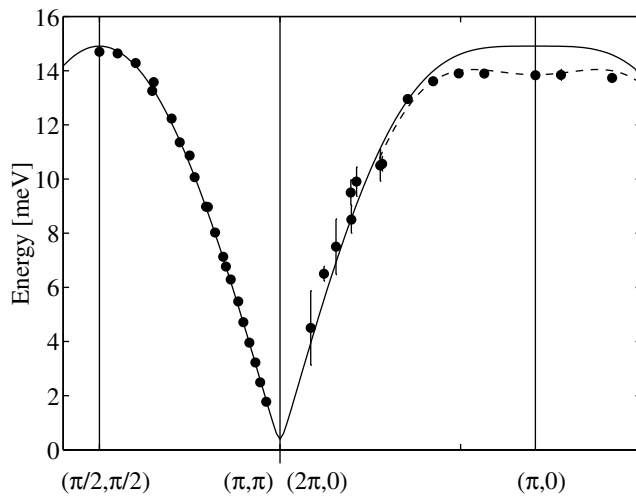


FIG. 2. The SW dispersion in CFTD at 8 K. The solid line is a fit of the $Q||[1, 1]$ part to nearest-neighbor SW theory, giving $J = 6.31 \pm 0.02$ meV. The dashed line is the result of an expansion from the Ising limit [13] using $J = 6.31$ meV.

Along $[1, 0]$ there is a pronounced dip in energy around $(\pi, 0)$, indicating a dispersion of $6\% \pm 1\%$ along the ZB from $(\pi/2, \pi/2)$ to $(\pi, 0)$. Such a ZB dispersion has also been observed in $\text{Sr}_2\text{Cu}_3\text{O}_4\text{Cl}_2$ [27], where it was explained in terms of the Ising-limit expansion [13]. Indeed, the Ising-limit expansion accounts perfectly for our data without any additional parameters (dashed line in Fig. 2). However, our data can equally well be modeled within SW theory by introducing an antiferromagnetic next-nearest-neighbor coupling of $(0.067 \pm 0.007) \times J$, and *a priori* the experimental data cannot be used to discriminate between these two possibilities. To help resolve this issue we have undertaken numerical computations on finite sized systems, and do indeed find a ZB dispersion for pure nearest-neighbor coupling [28]. QMC on lattices up to 32×32 spins and temperatures down to $0.3J$ extrapolate to about 6% ZB dispersion [29]. Exact diagonalization of an $\sqrt{32} \times \sqrt{32}$ system displays a ZB dispersion of 4.8%. Both techniques yield no ZB dispersion in the 4×4 system, which indicate that a significant number of spins are involved in this effect. We conclude that the experimentally observed ZB dispersion is indeed an intrinsic quantum effect on the $T = 0$ spin dynamics of the pure 2DQHAFSL model with nearest-neighbor interactions. Recently a ZB dispersion of -13% (i.e., opposite sign) has been found

in La_2CuO_4 , which is attributed to higher-order spin couplings [30].

Above T_N , the magnetic excitation spectrum broadens, making it more difficult to distinguish from the phonon scattering. To determine the phonon scattering, the SW contribution was simulated by convolving the linear SW result with the experimental resolution. When subtracted from the 8 K data the remaining intensity is dominated by phonon scattering. This was scaled to the thermal population factor and subtracted from the remaining $T > T_N$ data. As this method assumes a uniformly renormalized SW dispersion, it obviously does not apply to $Q||[1, 0]$, and hence only the $Q||[1, 1]$ data were analyzed in this way. Figures 1(c) and 1(d) show examples of data sets where the phonon contributions have been removed. The background corrected data were analyzed by fitting cuts along energy to the same parametrization as for the 8 K data, but with the delta function replaced by the damped harmonic oscillator (DHO) line shape $\delta(\omega - \omega_Q) \rightarrow \frac{4}{\pi} \frac{\Gamma \omega_Q \omega}{(\omega^2 - \omega_Q^2)^2 + 4\Gamma^2 \omega^2}$. No clear trends could be found within error for the Q dependence of the fitting parameters A , \bar{J} , and $\bar{\Gamma}$. In the following we therefore choose to discuss the Q averaged values $\bar{A}(T)$, $\bar{J}(T)$, and $\bar{\Gamma}(T)$.

The amplitude, $\bar{A}(T) = \frac{2}{3} \left(\frac{\gamma e^2}{mc^2} \right)^2 Z_\chi S$, can be used to extract the renormalization $Z_\chi(T)$ of the susceptibility. (The factor $\frac{2}{3}$ becomes $\frac{1}{2}$ for the horizontal banks below T_N where the moments order almost vertically.) The temperature dependence of $Z_\chi(T)$ is listed in Table I. At low T , the experimental value is in perfect agreement with the predicted value of 0.51 [1]. At higher T , Z_χ appears to decrease, but no clear predictions for the T dependence of this quantity have yet been reported.

The uniform SW renormalization of ω_Q found along $[1, 1]$ at 8 K justifies the use of the average $\bar{J}(T)$, which divided by J gives the temperature-dependent SW renormalization $Z_c(T)$ as shown in Fig. 3. Kaganov and Chubukov [31] have calculated the temperature dependence of the higher-order quantum corrections to SW theory, obtaining $v_s(T) = v_s(0) \left[1 + \frac{\zeta(3)}{4\pi} \left(\frac{T}{T_N} \right)^3 \right]^{-1}$, where $\zeta(3) \approx 1.2021$. This result is represented by the solid line and is in good agreement with our data. The new QMC results are indicated by triangles and are also consistent with the data.

Various calculations of the SW damping all predict a Q dependence with a minimum at (π, π) . Around this point, the value of $\bar{\Gamma}$ is quite dependent on the definition of the line shape. This complication is irrelevant for

TABLE I. Temperature dependence of the susceptibility and SW velocity renormalization parameters, Z_χ and Z_c , and the SW damping $\bar{\Gamma}(T)/J$. Z_c has been normalized to match the theoretical value 1.18 at 8 K. The 8 K data were resolution limited, and therefore correspond to zero SW damping.

T (K)	8.0	16.2	20.9	25.6	30.4	36.2	45.1
Z_χ	0.51(4)	0.49(2)	0.51(2)	0.49(2)	0.42(3)	0.58(5)	0.41(8)
Z_c	1.18	1.19(1)	1.17(1)	1.17(1)	1.14(2)	1.07(4)	1.03(4)
$\bar{\Gamma}/J$	0.00(2)	0.08(1)	0.12(1)	0.17(2)	0.24(3)	0.38(5)	0.42(7)

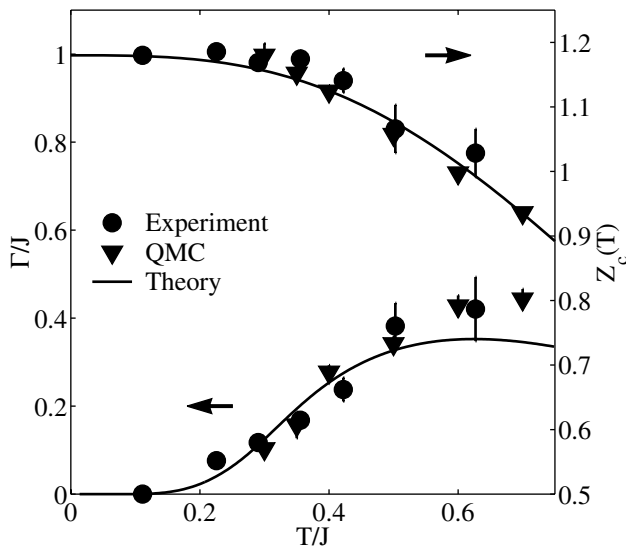


FIG. 3. The SW softening $Z_c = \tilde{J}/J$ and damping Γ/J as functions of temperature. The experimental data (circles) and new QMC results (triangles) are averages for $\omega > 2$ meV. The solid lines are, respectively, the prediction of Kaganov and Chubukov [31] for $Z_c(T)$ and the relation $\Gamma(T) = v_s(T)/\xi(T)$ for the damping.

the experimental data, where due to the large incoherent background, the fits were restricted to $\omega > 2$ meV $\approx J/3$. The experimentally determined SW damping is shown in Fig. 3. QMC results for the damping have been reported for $0.35 < T/J < 0.5$ [22]. We find that these overestimate the experimental values of $\tilde{\Gamma}$ by almost a factor of 2. To resolve this discrepancy, we have repeated the QMC calculations [28]. If the same maximum entropy method is used for analytic continuation of the imaginary time MC data, then the results of Ref. [22] are reproduced. We found, however, that it is more robust to impose the same DHO line shape as used to analyze our experimental data. When this is done the QMC values shown in Fig. 3 are obtained which are in good agreement with the experimental data. Scaling arguments have also been used to calculate the SW damping [14]. Since this approach mainly applies to the low-energy, long-wavelength behavior of the system which was not probed in our experiments, we believe that it is not appropriate to compare it with our data. We do note, however, that for $T < J/2$ the data lie above the prediction for $Q = (\pi, \pi)$, and below the prediction extrapolated to $Q = (\pi/2, \pi/2)$. Our result for $\Gamma(T)$ differs from those extracted from NMR in $\text{Sr}_2\text{CuCl}_2\text{O}_2$ [23]. This may be because NMR is a local probe in the low-energy limit, and the result for $\Gamma(T)$ relies on a global assumption for $S(Q, \omega)$. In contrast, our data give a direct and assumption-free measurement of $\Gamma(T)$.

Spin waves are eigenmodes with respect to antiferromagnetic order and vary on a length scale set by the correlation length $\xi(T)$. The most naive way to estimate the lifetime of a SW would be to divide $\xi(T)$ [12] by the SW

velocity $v_s(T)$ [31]. In Fig. 3 the solid line is the inverse lifetime $\Gamma(T) = v_s(T)/\xi(T)$ obtained in this way, and is seen to be in surprisingly good agreement with the data.

In summary, we have measured the excitation spectrum of CFTD, which is an excellent physical realization of the 2DQHAFSL. Combining our data and numerical calculations, the existence of a quantum induced ZB dispersion has been unambiguously established. The finite temperature behavior has been probed up to $T > J/2$, where well-defined SW-like excitations persist. The temperature dependence of the SW softening and damping in this strongly quantum mechanical system are remarkably well described, without any adjustable parameters, by existing theories based on a quantum renormalization of the classical system.

We gratefully acknowledge Rajiv R. P. Singh for useful discussions. This work was supported by the Danish Research Academy, the U.K. EPSRC, and the EU through its TMR and IHP programmes. ORNL is managed for the U.S. DOE by UT Battle, LLC, Contract No. DE-AC05-00OR22725.

- [1] J. Igarashi, Phys. Rev. B **46**, 10 763 (1992).
- [2] S. Chakravarty *et al.*, Phys. Rev. B **39**, 2344 (1989).
- [3] J.-K. Kim *et al.*, Phys. Rev. Lett. **80**, 2705 (1998).
- [4] B. B. Beard *et al.*, Phys. Rev. Lett. **80**, 1742 (1998).
- [5] N. Elstner *et al.*, Phys. Rev. Lett. **75**, 938 (1995).
- [6] A. Cuccoli *et al.*, Phys. Rev. Lett. **79**, 1584 (1997).
- [7] K. Yamada *et al.*, Phys. Rev. B **40**, 4557 (1989).
- [8] R. J. Birgeneau *et al.*, Phys. Rev. B **59**, 13 788 (1999).
- [9] M. Greven *et al.*, Z. Phys. B **96**, 465 (1995).
- [10] H. M. Rønnow *et al.*, Phys. Rev. Lett. **82**, 3152 (1999).
- [11] P. Carretta *et al.*, Phys. Rev. Lett. **84**, 366 (2000).
- [12] P. Hasenfratz, Eur. Phys. J. B **13**, 11 (2000).
- [13] R. R. P. Singh *et al.*, Phys. Rev. B **52**, R15 695 (1995).
- [14] S. Tyč *et al.*, Phys. Rev. Lett. **62**, 835 (1989).
- [15] A. Auerbach *et al.*, Phys. Rev. Lett. **61**, 617 (1988).
- [16] M. Takahashi, Phys. Rev. B **40**, 2494 (1989).
- [17] A. Sokol *et al.*, Phys. Rev. Lett. **76**, 4416 (1996).
- [18] A. Sherman *et al.*, Phys. Rev. B **60**, 10 180 (1999).
- [19] S. Winterfeldt *et al.*, Phys. Rev. B **56**, 5535 (1997).
- [20] T. Nagao *et al.*, J. Phys. Soc. Jpn. **67**, 1029 (1998).
- [21] Y.-J. Wang *et al.*, Phys. Rev. B **56**, 10982 (1997).
- [22] M. Makivić *et al.*, Phys. Rev. Lett. **68**, 1770 (1992).
- [23] K. R. Thurber *et al.*, Phys. Rev. Lett. **79**, 171 (1997).
- [24] S. J. Clarke *et al.*, Solid State Commun. **112**, 561 (1999).
- [25] K. Yamagata *et al.*, J. Phys. Soc. Jpn. **50**, 421 (1981).
- [26] N. Burger *et al.*, Solid State Commun. **34**, 883 (1980).
- [27] Y. J. Kim *et al.*, Phys. Rev. Lett. **83**, 852 (1999).
- [28] H. M. Rønnow *et al.* (to be published).
- [29] O. F. Syljuåsen *et al.*, J. Phys. C **12**, L1 (2000).
- [30] R. Coldea *et al.*, cond-mat/0006384 (unpublished).
- [31] M. I. Kaganov *et al.*, in *Spin Waves and Magnetic Excitations*, edited by A. S. Borovik-Romanov *et al.* (North-Holland, Amsterdam, 1988), Vol. 22.2, p. 1. See also [32].
- [32] N. Elstner *et al.*, Phys. Rev. B **51**, 8984 (1995).